JOURNAL OF MATERIALS SCIENCE **38** (2003) 427–435

Optimization of the preparation conditions of polygranular carbons from mesophase

F. FANJUL, M. GRANDA*, R. SANTAMARÍA, R. MENÉNDEZ
Instituto Nacional del Carbón, CSIC. C/Francisco Pintado Fe, 26, 33011-Oviedo, Spain
E-mail: mgranda@incar.csic.es

Polygranular carbons were prepared from a coal-tar pitch based mesophase by sintering, using different experimental conditions. The temperature and time of mesophase stabilization, the pressure applied during moulding, and the sintering heating rate were investigated in order to obtain materials with optimum properties. Oxidative stabilization with air between 225 and 250°C causes a significant reduction in the plasticity of the coal-tar pitch based mesophase, allowing moulding and sintering to be performed. An increase in the moulding pressure results in an increase in the bulk density of the green materials. However, sintering must be carried out at low heating rates in order to control the release of gases and thus avoid damage to the sintered material. Higher sintering heating rates are compatible with low moulding pressures and a high degree of stabilization. Whenever the materials do not distort during sintering, a common feature observed is that mechanical and electrical properties improve with increasing moulding pressure, while an increase in sintering heating rate only serves to improve the strength of the materials.

1. Introduction

Polygranular graphites are high-density materials that have applications in many fields, where outstanding electrical, mechanical and thermal properties are required (nuclear reactors, electrical discharge machining, semiconductors, carbon brushes [1, 2]). These types of graphites can be obtained according to a procedure similar to that described in graphite electrode technology, using pulverized petroleum coke as filler and pitch as binder [1]. This process presents serious disadvantages. Firstly, multiple densification cycles must be used to achieve the desired density and electrical/mechanical properties. Secondly, carbonization/graphitization have to be carried out at low heating rates. Consequently, the process is expensive and long periods of time are required. These drawbacks can be overcome by using carbonaceous mesophase as a graphite precursor [1, 3–11]. Mesophase is able to sinter without any external binder. Moreover, the great packing capacity of mesophase during carbonization/graphitization results in a high-density material, which does not require further densification. This leads to a simplification of the process and a substantial reduction in operation costs. Additionally, it has been proved that mesophase-derived graphites have better properties than polygranular graphites obtained by the traditional procedure [1].

Carbonaceous mesophase occurs as an intermediate phase during the carbonization of some organic precursors, such as pitches [12]. When an isotropic pitch is heated, it polymerizes and passes through a liquid crystal phase, called mesophase [12]. As the temperature increases, more mesophase is formed from the isotropic pitch. This process continues until the entire pitch has been transformed into coalesced mesophase. However, it is possible to interrupt the carbonization at a stage when mesophase is in the form of microspheres, which coexist with isotropic pitch. Solvent extraction [10, 13, 14] and centrifugation [15, 16] are the most widely used techniques for the separation of these two phases.

Blanco *et al*. [17] have recently described a simple and economic procedure for the separation of the mesophase in thermally treated coal-tar pitch. This procedure, based on filtration, yields two raw materials with different properties [18–20] and different applications. The isotropic fraction has been successfully used for the preparation of general purpose carbon fibres [21, 22], while the mesophase, in the form of microspheres of homogeneous size, is endowed with excellent sintering properties after oxidative treatment [23, 24].

The present work deals with the feasibility of this mesophase as a mean of preparing high-density polygranular carbons, as a previous step to the preparation of polygranular graphites. Parameters related with the preparation of the carbons, such as stabilization temperature and soaking time, moulding pressure and sintering heating rate, have been optimized. The microstructure of the polygranular carbons was studied by optical microscopy and their properties by means of flexural strength and electrical resistivity.

*Author to whom all correspondence should be addressed.

2. Experimental

2.1. Polygranular carbon precursors

A coal-tar pitch based mesophase (M-A) was used as precursor for the preparation of the polygranular carbons. M-A was obtained from an impregnating-grade coal-tar pitch, by thermal treatment at 430°C for 4 h. The thermally treated pitch, containing 32.3 vol% of mesophase, was then filtered in order to concentrate the mesophase. Filtration was carried out at 300–350°C with the aid of a nitrogen pressure of 0.5 MPa, using a 25 μm wire-cloth filter [17]. The resultant residue (M-A) contained 86.6 vol% of mesophase microspheres.

Prior to sintering, the mesophase was stabilized with air at 225 and 250°C, using a multi-step temperature/time profile described elsewhere in a previous work [25]. In summary, powdered mesophase, ground and sieved to <200 μm, was heated in an oven under an air-rich atmosphere at 5°C min^{-1} to 200°C, this temperature being maintained for 1 h. Then, it was heated at 1°C min^{-1} to 225 for 1 (M-A225/1) and 2 h (M-A225/2), and thereafter at 1°C min^{-1} to 250°C for 1 h (M-A250/1).

2.2. Characterization of the precursors

Elemental analysis of the parent and stabilized samples was carried out using a LECO CHNS-932 microanalyzer. Oxygen was determined directly in a LECO-VTF900 graphite furnace.

Toluene insolubles were calculated adopting the Pechiney B-16 (series PT-7/79 of STPTC) standard. 1-methyl-2-pyrrolidinone (NMP) insolubles were determined in a similar way to quinoline insolubles (ASTM D2318 standard) but using NMP instead of quinoline.

The thermoplasticity of the samples was determined by means of a specifically designed device (Fig. 1), following a procedure similar to a thermomechanical analysis. The device was equipped with a stainless steel cell (10 mm in height and 9.7 mm i.d.) and a vertical stainless steel push rod (4.5 g) with a conical push rod tip (cone angle 30°). The displacement of the push rod was measured with an LVDT transducer, which detected variations of 1 μm. No external force was used to facilitate the entry of the push rod into the sample. 300 mg of sample, ground and sieved to <200 μm, was shaped into cylindrical pellets (9.6 mm i.d. and 5.0 mm height) by applying a uniaxial pressure of 140 MPa. The pellets were then placed in the cell and heated at 5°C min^{-1} to 430°C in a nitrogen flow of 20 L h^{-1}. The curves recorded the variation of the penetration of the conical push rod into the pellet with temperature.

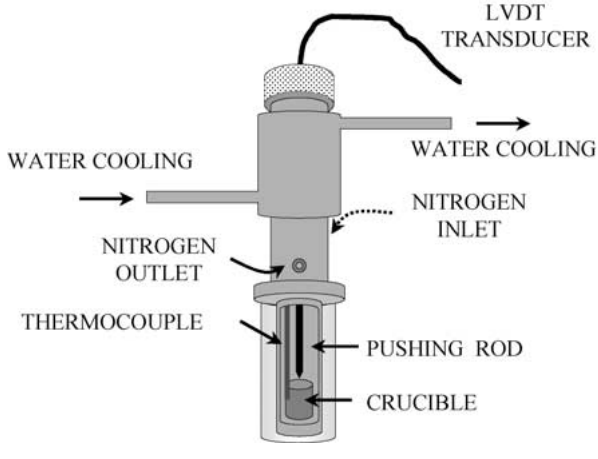

Figure 1 Experimental device used for determination of plasticity in the mesophases.

Thermogravimetric analysis (TG/DTG) was performed in a TA Instruments thermal analyzer. About 16 mg of sample (<200 μm of particle size) was placed in a platinum crucible (4.0 mm in height and 6.6 mm i.d.) and heated to 1000°C at 10°C min^{-1} in a nitrogen flow of 150 mL min^{-1}.

Optical microscopy was performed on polished cross-sections of parent mesophase (M-A) embedded in epoxy resin, using a polarized-light microscope. The microscope was equipped with a 1-λ retarder plate to generate interference colours. Representative micrographs of the sample were taken using oil-immersion objectives of $\times$20 and $\times$50 magnifications. The size distribution of microspheres in M-A was studied by means of an automatic microanalyser, using an oil-immersion objective $\times$20. This device allowed fields of 316 $\times$ 240 μm to be captured. The size distribution of the microspheres was given after analysing an average of 700 units.

2.3. Preparation of the polygranular carbons

Stabilized mesophase samples (M-A225, M-A250) were finely pulverized in a laboratory centrifugal ball mill, operating at 300 rpm for 10 and 30 min. The rotation was reversed every one minute. $\sim$30 g of sample was placed in a grinding jar, along with 30 mL of dispersant agent (acetone/isopropanol: 50/50 vol%) to facilitate the milling of the sample. After milling, the powdered samples were dried and moulded into prismatic specimens (50 $\times$ 10 $\times$ 3–4 mm) by the application of two different uniaxial mechanical pressures (50 and 80 MPa). The green materials were then sintered at 1000°C following four different programs: (i) at 1°C min^{-1} from room temperature to 200°C, at 0.3°C min^{-1} from 200 to 300°C, at 0.1°C min^{-1} from 300 to 550°C, at 0.3°C min^{-1} from 500 to 1000°C, and after 30 min at 1000°C at 1°C min^{-1} from 1000 to 550°C; (ii) the same program but heating at 0.3°C min^{-1} from 300 to 550°C; (iii) heating and cooling at 1°C min^{-1}; and finally (iv) heating and cooling at 5°C min^{-1}. Fig. 2 summarizes the sequence of steps used to prepare polygranular carbons from powdered mesophase.

2.4. Characterization of the polygranular carbons

The particle size distribution in the powdered mesophase was determined in a Coulter LS-130 equipment, using water as dispersant medium.

The bulk density (d_b) in the green and sintered materials (polygranular carbons) was calculated by measuring the dimensions and the weight of representative

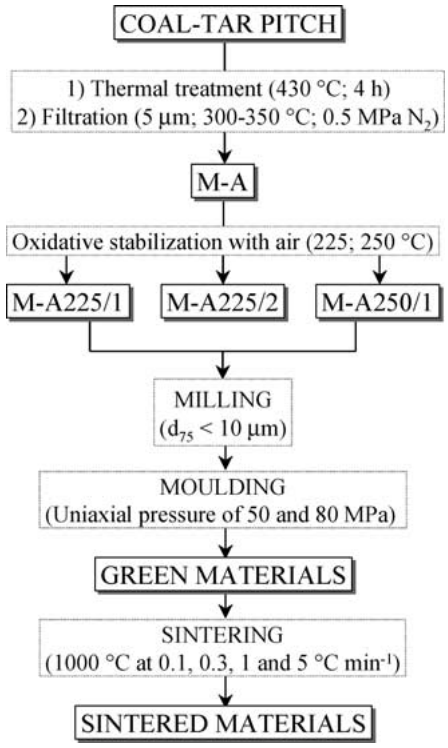

Figure 2 Sequence of steps involved in the preparation of polygranular carbons from mesophase.

samples. Density in water (d_{H_2O}) was determined according to the ASTM C20 standard, using specimens of $40 \times 8 \times 3$ mm. Specimens of $20 \times 8 \times 3$ mm were used in the determination of density by helium pycnometry (d_{He}). The porosity, determined as the access of water (P_{H_2O}) and helium (P_{He}) to the pores, was calculated from Equations 1 and 2, respectively:

$$P_{H_2O} = 100 \cdot (d_b/d_{H_2O}) \quad (1)$$

$$P_{He} = 100 \cdot (d_b/d_{He}) \quad (2)$$

Flexural strength was determined by a four-point-bending test, according to the ASTM C651 standard. Specimens of 40×83 mm were tested in a four-point rig over a span of 21 mm between 5-mm-diameter supported rollers. The load was applied by means of two 5-mm-diameter loading rollers separated 10 mm from each other. The machine cross-head speed was 1 mm min^{-1}. The results were quoted as the mean of values from 3 specimens of each material.

Electrical resistivity was measured at room temperature, using a laboratory-designed device. This device consists of two parallel copper plates (35×40 mm) connected to a power supply, which was allowed to operate to an intensity of 1 A. Prismatic specimens of $20 \times 8 \times 3$ mm were fitted between the two copper plates. The voltage drop between two points of the specimens was measured by two pins separated 10 mm from each other and recorded in a multimeter. The electrical resistivity, quoted as the mean of 4 measurements on 3 specimens per sample, was calculated as follows (3):

$$\rho = (V \cdot s)/(I \cdot d) \quad (3)$$

where ρ, is the electrical resistivity (Ω m); V, the voltage (V); s, the cross-section of the specimen (m^2); I, the intensity (A); and d, the distance between the points of measurement (m).

The microstructure of the polygranular carbons was studied by optical microscopy in a similar way to that described in section 2.2.

3. Results and discussion

3.1. Characterization of polygranular carbon precursors

The coal-tar pitch based mesophase used in this study is mainly composed of microspheres (Fig. 3), and to a lesser extent, of isotropic material (13.4 vol%). The microspheres cover a range of diameters from <10 to 60 μm (Fig. 3). However, more than 82 vol% of the microspheres had a mean diameter of between 10 and 30 μm.

In contrast with the solvent extraction procedures used to separate mesophase, the filtration procedure to obtain M-A does not remove light compounds. These compounds are not only trapped in the isotropic material, which is present in small amounts, but also in the mesophase microspheres [19]. It is not surprising, therefore, that M-A is partially soluble in toluene and 1-methyl-2-pyrrolidinone (Table I). These compounds presumably confer a certain plasticity to the sample, allowing conformation to take place. However, when M-A is finely pulverized and moulded, the resultant specimens completely deform during subsequent sintering (Fig. 4). This shows that plasticity in the parent mesophase is excessively high.

The elemental analysis shows that the parent mesophase is mainly composed of carbon and hydrogen (Table I). Although the hydrogen is mostly aromatic, as

TABLE I Characteristics of parent and stabilized mesophase

Sample	H[a]	O[b]	C/H[c]	C/O[d]	NMPI[e]	TI[f]	I_{Ar}[g]
M-A	3.46	1.04	2.28	120.44	61.4	74.0	0.719
M-A225/1	3.31	3.15	2.33	38.92	69.3	90.8	0.786
M-A225/2	3.23	3.36	2.39	36.40	71.2	94.0	0.793
M-A250/1	3.14	4.05	2.44	29.99	74.6	97.9	0.816

[a]Hydrogen content (wt%).
[b]Oxygen content (wt%).
[c]Carbon/hydrogen atomic ratio.
[d]Carbon/oxygen atomic ratio.
[e]1-methyl-2-pyrrolidinone insolubles (wt%).
[f]Toluene insolubles (wt%).
[g]Aromaticity index, determined by FTIR.

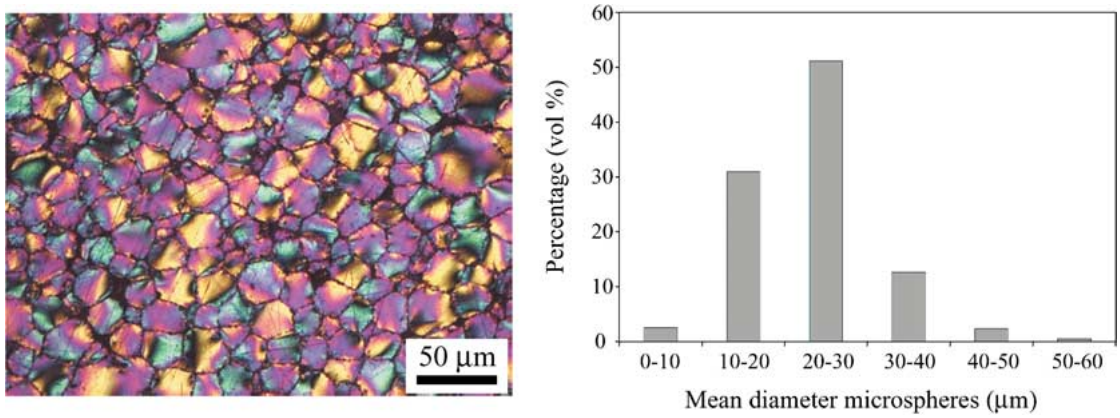

Figure 3 Optical micrograph of a cross-section (left) and microsphere mean diameter (right) of the parent mesophase.

Figure 4 Macroscopic appearance of parent mesophase (a) before and (b) after sintering to 1000°C.

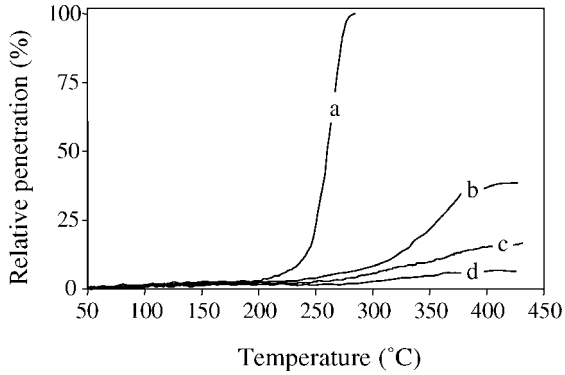

Figure 5 Variation of relative penetration with temperature for (a) M-A, (b) M-A225/1, (c) M-A225/2 and (d) M-A250/1.

revealed by the high aromaticity index determined by infrared spectroscopy, the contribution of the aliphatic hydrogen is by no means negligible (Table I). This suggests that plasticity might be reduced by oxidative stabilization with air at moderate temperatures. Indeed, when M-A is oxidatively stabilized, a substantial reduction in plasticity is achieved (Fig. 5). The significant decrease in hydrogen and increase in oxygen (Table I) indicates that oxidative stabilization is a dehydrogenative process. Hydrogen is removed as H_2O and oxygen uptake, giving rise to different oxygen-containing functional groups [25]. Aliphatic hydrogen is preferentially consumed against aromatic hydrogen [25]. Consequently, the aromaticity index increases with the severity of stabilization (Table I).

On the basis of the results obtained in previous studies [26], M-A was stabilized at 225 for 1 and 2 h (M-A225/1 and M-A225/2) and at 250°C for 1 h (M-A250/1). As mentioned above, stabilization is accompanied by an important reduction in the plasticity of the samples, determined as relative penetration (Section 2.2). In the parent mesophase relative penetration is completed below 270°C, the range of temperature needed to increase the penetration from 10 to 90% being 36°C. Plasticity is very sensitive to air treatment [13, 25, 26]. Thus, stabilization at 225°C for 1 and 2 h produces a significant reduction in relative penetration (38.5 and 16.7%, respectively). At higher temperatures (250°C) penetrability is only 6.6%. It should be noted that under the experimental conditions used in this study, the increase in the stabilization temperature from 225 to 250°C causes a greater reduction in plasticity than prolongation of the stabilization by 1 h at 225°C, which is in agreement with the oxygen uptake and hydrogen removed from the samples (Table I).

The three stabilized samples were used for the preparation of polygranular carbons. Observations carried out by optical microscopy showed that oxidative stabilization did not cause any modification to the microcrystallite size of the stabilized samples, isolated microspheres being the main microstructural feature.

3.2. The effect of moulding pressure and sintering heating rate on the structure and properties of polygranular carbons

Prior to be moulded into prismatic specimens, the stabilized mesophase was finely pulverized. The three stabilized samples exhibit a similar particle size distribution (Fig. 6). When milling is performed for 10 min, the particle size distribution falls within a range, which varies from 0.1–40 μm, d_{75} and d_{90} being <10 and <17 μm, respectively. The prolongation of the milling up to 30 min causes only a slight shift to a smaller particle size. This clearly reveals that 10 min is enough time to achieve a good milling of the samples.

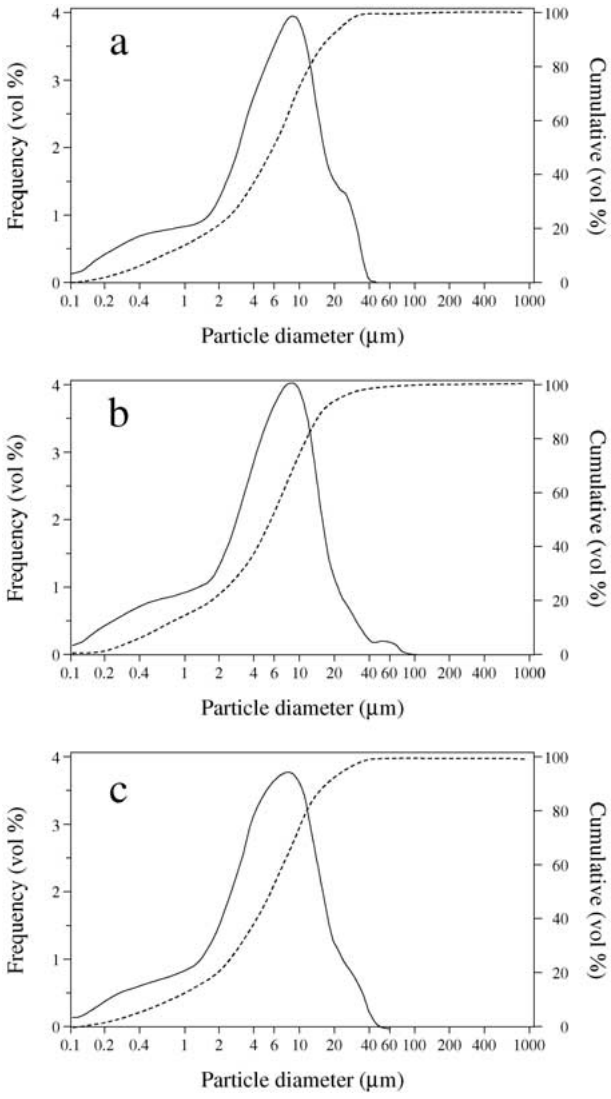

Figure 6 Particle size distribution of stabilized mesophase after 10 min of milling: (a) M-A225/1, (b) M-A225/2 and (c) M-A250/1.

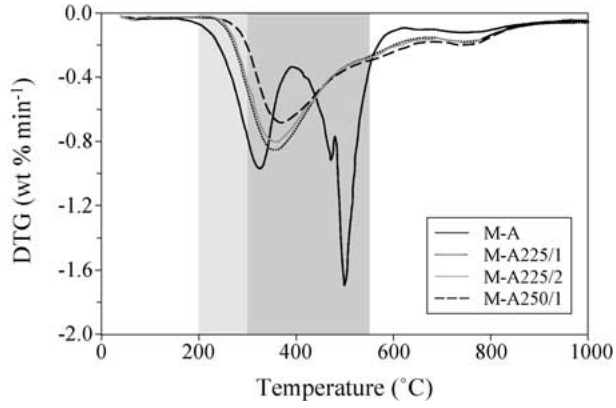

Figure 7 DTG curves of parent and stabilized mesophases.

Table II summarizes the main properties of the polygranular carbons prepared from M-A225/1, M-A225/2 and M-A250/1 under different moulding pressures and sintering heating rates. The pressure applied for moulding and the sintering heating rate have an important effect on the properties of the carbons. The heating rate is of special relevance because the major variations in weight loss in the parent mesophase, as well as in the stabilized mesophase, occur within certain ranges of temperature. The thermogravimetric derivative curves of the samples show that weight loss starts above 200°C (Fig. 7). The loss increases between 300 and 550°C, but then occurs with less intensity after 550°C. These results provide valuable information for deciding on the sequence of sintering heating rates in order to minimize the effects of the removal of gases in the structure of the resultant materials. For this reason, the heating rate from 200 to 550°C was carefully controlled, especially in the 300 and 550°C temperature range. When sintering is performed at 5°C min^{-1}, the resultant carbons show significant internal (large pores and cracks) and external (bloating) imperfections. This is because the heating rate is too high and the release of gases occurs within a short interval of time, thereby damaging the material. Likewise, moulding pressures of 80 MPa lead to distorted materials, except in the case of M-A250/1. All the precursors were, therefore, moulded at 50 MPa, M-A250/1 being moulded at 50 and 80 MPa. To compensate for the increase in moulding pressure from 50 to 80 MPa in M-A250/1, sintering must be performed at low heating rates (0.1 and 0.3°C min^{-1} between 300 and 550°C). This is because of the gases released during sintering. It has been observed that with the increase of moulding pressure, the bulk density of green materials increases (Table II), but at the same time, the network of voids that allows the diffusion of gases produced during sintering is reduced. Consequently, gases need to find new pathways for release, causing dramatic damage to the resultant sintered materials. A common feature in distorted material is that these materials usually undergo a lower weight loss during sintering than non-distorted materials (Table II).

The weight loss, volumetric contraction and densities of polygranular carbons hardly change with the degree of stabilization in the precursors (Table II). However, more detailed observation shows that for non-distorted carbons, which are prepared under the same moulding pressure, the weight loss increases while the volumetric contraction decreases with the severity of stabilization. Moreover, the greater the plasticity of the precursor, the greater the volumetric contraction and bulk density of the materials. In contrast, water and helium densities follow the opposite trend to bulk density. Consequently, a decrease in plasticity, produced by a severer stabilization, causes an increase in the amount of water and helium porosities. A comparison of the materials prepared under different moulding pressures (M-A250/1 moulded at 50 and 80 MPa) shows that an increase in pressure produces an increase in bulk density and a decrease in weight loss, volumetric contraction and water and helium densities. The amount of water and helium porosities, therefore, is substantially reduced (Table II). These results suggest that an increase in moulding pressure is beneficial for the structural parameters of the material. However, an excess of pressure can result in bloating during subsequent sintering, as occurs in polygranular carbons from M-A225/1 and M-A225/2 when they are moulded at 80 MPa.

The relative increase in bulk density, determined as the carbon bulk density/green bulk density ratio, could be considered as a useful way to measure the

TABLE II Main characteristics of polygranular carbons

Sample	Green materials			Sintered Materials								
	P[a]	r[b]	d_{bo}[c]	$-\Delta W$[d]	$-\Delta V$[e]	d_b[f]	d_{H_2O}[g]	d_{He}[h]	d_b/d_{bo}[i]	P_{H_2O}[j]	P_{He}[k]	ρ[l]
M-A225/1	50	0.1	1.098	18.79	37.04	1.423	1.806	1.977	1.30	21.21	28.02	55.8
		0.3		18.10	36.66	1.419	1.811	1.960	1.29	21.65	27.60	57.3
		1		14.90				Distorted material				
	80	0.1	1.162	16.08				Distorted material				
M-A225/2	50	0.1	1.105	19.54	36.75	1.404	1.854	1.988	1.27	24.27	29.38	53.0
		0.3		18.80	37.15	1.428	1.829	1.973	1.29	21.92	27.62	58.9
		1		19.19				Distorted material				
	80	0.1	1.193	17.92				Distorted material				
M-A250/1	50	0.1	1.109	19.74	35.52	1.397	1.853	2.024	1.26	24.60	30.99	57.0
		0.3		19.02	35.26	1.392	1.837	1.984	1.26	24.21	29.84	–
		1		18.37	35.65	1.392	1.826	1.965	1.26	23.77	29.16	61.6
		5		15.30				Distorted material				
	80	0.1	1.168	18.66	34.64	1.430	1.809	1.949	1.22	20.95	26.62	51.3
		0.3		18.28	34.36	1.428	1.789	1.916	1.22	20.18	25.49	56.5
		1		19.22				Distorted material				

[a]Moulding pressure (MPa).
[b]Carbonization heating rate between 300 and 550°C (°C min^{-1}).
[c]Green bulk density (g cm^{-3}).
[d]Weight loss (%).
[e]Volume shrinkage (%).
[f]Bulk density (g cm^{-3}).
[g]Density in water (g cm^{-3}).
[h]Density in helium (g cm^{-3}).
[i]Relative bulk density.
[j]Porosity accessible to water (vol%).
[k]Porosity accessible to helium (vol%).
[l]Electrical resistivity ($\mu\Omega$ m).

self-densifying capacity of the precursor during sintering. The severity of stabilization reduces the capacity of the precursor for self-densification (Table II). This could be related to the loss of sinterizability due to the reduction in plasticity of the precursor.

Fig. 8 shows optical micrographs of cross-sections of the polygranular carbons obtained at different sintering heating rates. Neither the moulding pressure nor the heating rate seem to have had a significant effect on the microstructure of the resultant carbons. However, the degree of stabilization does play an important role in the development of porosity. The mesophase stabilized at 250°C gives rise to polygranular carbons with lower porosity (Fig. 8c and d), detectable under a microscope, than mesophases stabilized at 225°C (Fig. 8a and b). Nevertheless, porosity is scarce, especially in the case of carbons from M-A250/1, pores being <5 μm in length. An important finding was that the small amount of isotropic material present in the stabilized mesophases remains isotropic in the polygranular carbons. Consequently, stabilization must modify the composition of the isotropic material in such a way that it cannot be converted into anisotropic material during sintering. The higher the temperature of stabilization, the more pronounced the modifications are. Thus, in polygranular carbons obtained from M-A250/1 pores are mainly located between grains (inter-grain pores, Fig. 8e, position A), whereas M-A225/1 and M-A225/2 give rise to carbons in which inter-grain pores coexist with pores located in isotropic grains (Fig. 8f, position B). This suggests that in M-A225/1 and M-A225/2 volatiles from the isotropic material are released during sintering to a greater extent than in M-A250/1. This is in agreement with what has just been said and the results of plasticity shown in Fig. 5.

The moulding pressure and sintering heating rate also have a significant effect on the mechanical properties of polygranular carbons (Fig. 9). Four-point flexural strength improves as the moulding pressure and sintering heating rates increase, the effect of pressure being more pronounced than the effect of the heating rate. An exception is the case of M-A225/1 (50 MPa) when it is sintered at 0.3°C min^{-1} between 300 and 550°C. A possible explanation for this is that M-A225/1 is the most plastic precursor, and consequently, requires low sintering heating rates to prevent bloating and other possible deformations. Braun and Hüttinger [27] found that at low temperatures of sintering, specimens with high plasticity could hinder the removal of gases. In our case, these occluded gases might have been released at higher temperatures producing structural imperfections. This is illustrated by the scanning electron images shown in Fig. 11 for M-A225/1 sintered at 0.1 and 0.3°C min^{-1}. At 0.1°C min^{-1}, M-A225/1 generates small-size pores (Fig. 10a, position A), which coexist with pores of a larger size (<5 μm). These large pores are mainly located in the isotropic material and are characterized by thick walls (Fig. 10a, position B). On the other hand, when M-A225/1 is sintered at 0.3°C min^{-1}, the large pores are frequently associated with microcracks (Fig. 10b, position C), which are presumably generated by the escape of the occluded gases. These microcracks could be the factor responsible for the above mentioned decrease in flexural strength.

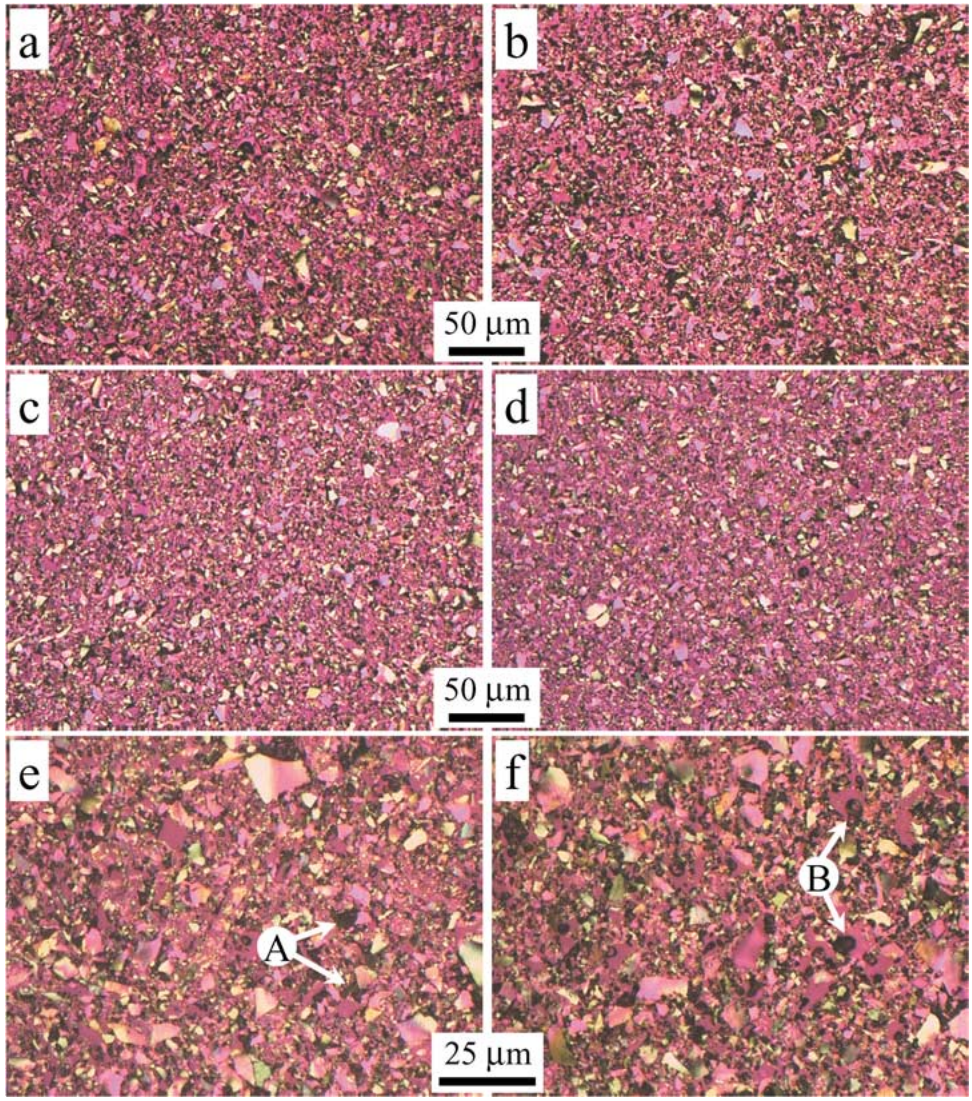

Figure 8 Optical micrographs of cross-sections of (a, f) M-A225/1 (50 MPa/0.1°C min^{-1}); (b) M-A225/2 (50 MPa/0.1°C min^{-1}); (c, e) M-A250/1 (50 MPa/0.1°C min^{-1}); and (d) M-A250/1 (80 MPa/0.1°C min^{-1}).

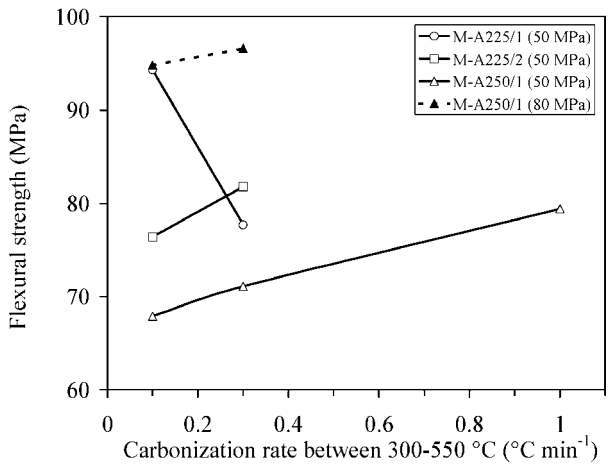

Figure 9 Variation of four-point flexural strength of polygranular carbons with moulding pressure and sintering heating rate between 300 and 550°C.

This relationship between the plasticity of precursor and the flexural strength is corroborated by the fact that under the same moulding pressure and the same sintering heating rate, M-A225/2 and M-A250/1, which are less plastic than M-A225/1, give rise to polygranular carbons with higher values of flexural strength. Moreover, it was found that there is a relationship between the four-point flexural strength of the materials and the amount of water and helium porosities (Fig. 11). Thus, the lower the porosity, the higher the flexural strength.

The effect of the preparation conditions on the electrical properties is also evident (Table II). The results show that the variations in electrical resistivity with moulding pressure and sintering heating rate do not follow the same trend, as in the case of flexural strength. An increase in moulding pressure produces a decrease in electrical resistivity (57.0 and 51.3 $\mu\Omega$ m, for M-A250/1 sintered at 0.1°C min^{-1} and moulded at 50 and 80 MPa, respectively), while with an increasing sintering heating rate the electrical resistivity increases in the resultant carbons (e.g. 57.0 and 61.6 $\mu\Omega$ m, for M-A250/1 moulded at 50 MPa and sintered at 0.1 and 1°C min^{-1}. At this point, it must be emphasized that it is mainly porosity that controls the properties of the polygranular carbons. The presence of pores causes a discontinuity for the conduction of electricity through the material. In general terms, electrical resistivity increases with the increase in the amount of pores accessible to water and helium (Table II).

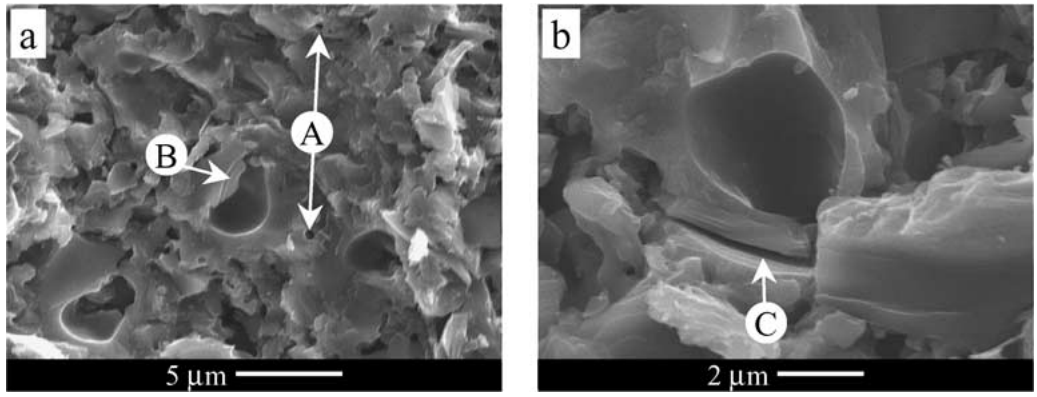

Figure 10 Scanning electron images of polygranular carbons obtained from M-A225/1 (50 MPa) sintered at (a) 0.1 and 0.3°C min^{-1}.

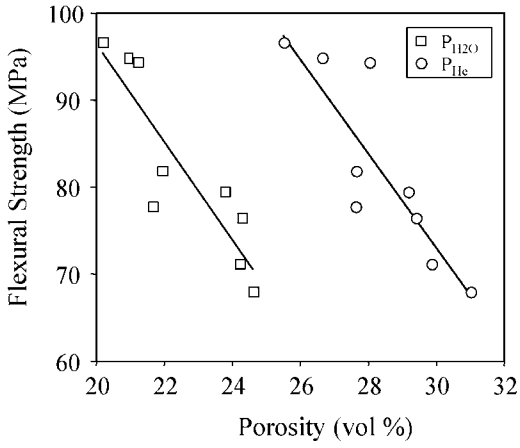

Figure 11 Variation of four-point flexural strength of polygranular carbons with porosity.

4. Conclusions

The sinterizability of a coal-tar pitch based mesophase is related with its plasticity. This property can be adjusted by oxidative stabilization, which depends primarily on temperature, but also on soaking time.

Under the conditions used in this study neither the moulding pressure nor the sintering heating rate have a relevant effect upon the micro-crystallite size of the resultant carbons. However, the degree of stabilization of the mesophase is of great importance for the development of porosity. Given the same moulding pressure and sintering heating rate, the severer the stabilization, the lower the amount of water and helium porosities in the material. Differences between water and helium densities and bulk density suggest that a substantial amount of porosity in the material corresponds to small-size pores.

The mechanical and electrical properties of carbons improve as the moulding pressure is increased. An increase in the sintering heating rate leads to an improvement of the flexural strength, but at the same time, increases the values of electrical resistivity.

Acknowledgements

The authors would like to thank CICYT-FEDER (Project Ref. 1FD1997-1657 MAT) for financial support.

References

1. A. OYA, in "Introduction to Carbon Technologies" (Publicaciones de la Universidad de Alicante, Alicante, 1997) p. 561.
2. R. WOLF in "Design and Control of Structure of Advanced Carbon Materials for Enhanced Performance" NATO Science Series: Vol. 374 (Kluwer Academic Publishers, Dordrecht, 2001) p. 217.
3. W. R. HOFFMANN and K. J. HÜTTINGER, *Carbon* **32** (1994) 1087.
4. I. MOCHIDA, R. FUJIURA, T. KOJIMA, H. SAKAMOTO and T. YOSHIMURA, *ibid.* **33** (1995) 265.
5. W. BOENIGK and D. SCHNITZLER, in Extended Abstracts of Carbon'96, Newcastle upon Tyne, July 1996 (British Carbon Group) Vol. 1, p. 22.
6. G. BATHIA, R. K. AGGARWAL, N. PUNJABI and O. P. BAHL, *J. Mater. Sci.* **32** (1997) 135.
7. J. SCHMIDT, K. D. MOERGENTHALER, K. P. BREHLER and J. ARNDT, *Carbon* **36** (1998) 1079.
8. Y. LÜ, L. LING, D. WU, L. LIU, B. ZHANG and I. MOCHIDA, *J. Mater. Sci.* **34** (1999) 4043.
9. Y. G. WANG, Y. KORAI and I. MOCHIDA, *Carbon* **37** (1999) 1049.
10. M. MARTÍNEZ-ESCANDELL, P. CARREIRA, M. A. RODRÍGUEZ-VALERO and F. RODRÍGUEZ-REINOSO, *Carbon* **37** (1999) 1662.
11. B. RAND and R. WOLF in "Design and Control of Structure of Advanced Carbon Materials for Enhanced Performance" NATO Science Series: Vol. 374 (Kluwer Academic Publishers, Dordrecht, 2001), p. 241.
12. J. D. BROOKS and G. H. TAYLOR, in "Chemistry and Physics of Carbon" (Marcel Dekker, New York, 1968) p. 243.
13. A. GSCHWINDT and K. J. HÜTTINGER, *Carbon* **32** (1994) 1105.
14. Y. G. WANG, Y. C. CHANG, S. ISHIDA, Y. KORAI and I. MOCHIDA, *ibid.* **37** (1999) 969.
15. L. S. SINGER, D. M. RIFFLE and A. R. CHERRY, *ibid.* **25** (1987) 249.
16. M. KODAMA, T. FUJIRUA, K. ESUMI, K. MEGURO and H. HONDA, *ibid.* **26** (1988) 595.
17. C. BLANCO, R. SANTAMARÍA, J. BERMEJO and R. MENÉNDEZ, *ibid.* **35** (1997) 1191.
18. C. BLANCO, O. FLEUROT, R. MENÉNDEZ, R. SANTAMARÍA, J. BERMEJO and D. EDIE, *ibid.* **37** (1999) 1059.
19. C. BLANCO, R. SANTAMARÍA, J. BERMEJO and R. MENÉNDEZ, *ibid.* **38** (2000) 1169.
20. C. BLANCO, V. PRADA, R. SANTAMARÍA, J. BERMEJO and R. MENÉNDEZ, *Journal of Analytical and Applied Pyrolysis* **63** (2002) 251.
21. V. PRADA, C. BLANCO, R. SANTAMARÍA, J. BERMEJO and R. MENÉNDEZ, in Extended Abstracts of 24th Biennial Conference on Carbon, Charleston, July 1999 (American Carbon Society) Vol. II, p. 374.
22. E. MORA, C. BLANCO, V. PRADA, R. SANTAMARÍA, M. GRANDA and R. MENÉNDEZ, *Carbon* **40** (2002) 2719.

23. F. FANJUL, M. GRANDA, J. BERMEJO and R. MENÉNDEZ, in Abstracts of Eurocarbon 2000, Berlin, July 2000 (Deutsche Keramische Gesellschaft e. V.) Vol. II, p. 501.
24. F. FANJUL, M. GRANDA, R. SANTAMARÍA, J. BERMEJO and R. MENÉNDEZ, *Journal of Analytical and Applied Pyrolysis* **58/59** (2001) 911.
25. F. FANJUL, M. GRANDA, R. SANTAMARÍA and R. MENÉNDEZ, *Fuel* **81** (2002) 2061.
26. *Idem*., *carbon*, in press.
27. M. BRAUN and K. J. HÜTTINGER, *ibid*. **34** (1996) 1473.

Received 1 May
and accepted 4 September 2002